1   **A new role of low barrier hydrogen bond in mediating protein stability by small**

2   **molecules**

3   Jianhong Yang[1#], Yong Li[1#], Qiang Qiu[1#], Ruihan Wang[2#], Wei Yan[1], Yamei Yu[1], Lu

4   Niu[1], Heying Pei[1], Haoche Wei[1], Liang Ouyang[1], Haoyu Ye[1], Dingguo Xu[2], Yuquan

5   Wei[1], Qiang Chen[1*], Lijuan Chen[1*]

6
7

8   [1] Laboratory of Natural and targeted small molecule drugs, State Key Laboratory of

9   Biotherapy and Cancer Center, National Clinical Research Center for Geriatrics, West

10   China Hospital, Sichuan University and Collaborative Innovation Center of

11   Biotherapy, Chengdu, 610041, China

12   [2] MOE Key Laboratory of Green Chemistry and Technology, College of Chemistry,

13   Sichuan University, Chengdu, Sichuan, 610064, China

14

15   [#]These authors equally contribute to this work.

16   Correspondence should be addressed to L.C. (email: chenlijuan125@163.com)

17   Additional corresponding authors: Q.C. (qiang_chen@scu.edu.cn).

18

19   ***Abstract***

20   Low barrier hydrogen bond (LBHB) is a special type of hydrogen bond which occurs

21   where two heteroatoms with similar p*Ka* values share a single proton resulting in an

22   unusually strong and short hydrogen bond. LBHBs in protein play important roles in

23   enzyme catalysis and maintaining protein structural integrity but its other biochemical

24   roles are unknown. Here we report a novel function of LBHB in selectively inducing

25   tubulin protein degradation. A tubulin inhibitor, 3-(3-Phenoxybenzyl) amino-β-

26   carboline (PAC), promotes selective degradation of αβ-tubulin heterodimers by binding

27   to the colchicine site of β-tubulin. Biochemical studies have revealed that PAC

28   specifically destabilizes tubulin, making it prone to aggregation that then predisposes it

29   to ubiquitinylation and then degradation. Structural activity analyses have indicated that

30   the destabilization is mediated by a single hydrogen bond formed between the pyridine

31   nitrogen of PAC and βGlu198, which is identified as a LBHB. In contrast, another two

32   tubulin inhibitors only forming normal hydrogen bonds with βGlu198 exhibit no

33   degradation effect. Thus, the LBHB accounts for the degradation. Most importantly, we

34   screened for compounds capable of forming LBHB with βGlu198 and demonstrated

35   that BML284, a Wnt signaling activator, also promotes tubulin heterodimers

36   degradation in a PAC-like manner as expected. Our study has identified a novel

37   approach for designing tubulin degraders, providing a unique example of LBHB

38   function and suggests that designing small molecules to form LBHBs with protein

39   residues resulting in the highly specific degradation of a target protein could be a new

40   strategy for drug development.

41

42   **Key words**: Tubulin degrader; Low barrier hydrogen bond; Drug design; Protein

43   stability; Protein degradation.

44

45   *1.Introduction*

46   Hydrogen bond was firstly discovered almost a century ago and it played an important

47   role in physics, chemistry and biology [1]. In life science, it is extremely important for

48   various biological processes, including the formation of DNA double helix structure,

49   protein secondary structure, protein folding and stability, enzyme catalysis, drugs

50   binding and molecular recognition [2-7]. A special hydrogen bond named low barrier

51   hydrogen bond (LBHB) was first proposed in 1990s [8, 9]. LBHB is distinguished from

52   conventional hydrogen bond by equally proton sharing between two heteroatoms [10].

53   These two heteroatoms usually have similar pKa values and form an unusually strong

54   and short ($\leq$2.65 Å for O-N pairs) hydrogen bond [3, 11, 12]. The proton of an LBHB

55   lies in the middle of the two heteroatoms and precise location of the proton by

56   experiment could provide direct evidence of existence of LBHB [13]. To locate the

57   proton of an LBHB in a protein can only be done by ultra-high-resolution (1.0 Å or less)

58   X-ray or neutron crystallography while it is technically difficult for most proteins [13].

59   Moreover, theoretical methods such as quantum mechanics/molecular mechanics

60   (QM/MM) calculation of potential-energy curves of proton has been widely used to

61   predict LBHB [13-15]. Formation of an LBHB can supply 10-20 kcal/mol energy which

62   can facilitate difficult biochemical reaction [9]. Thus, LBHB is regarded to be

63   responsible for catalytic efficiencies of several enzymes including aspartate

64   aminotransferase, ketosteroid isomerase, citrate synthase, serine proteases and

65   aminoglycoside-N3-acetyltransferase Via [16-20]. Besides, LBHBs are needed to

66   maintain protein structural integrity in proteins including rhamnogalacturonan

67   acetylesterase D192N mutant and human transketolase [21, 22]. However, other

68   biochemical roles of LBHBs are rarely reported.

69   LBHBs is also formed between small-molecule ligand and proteins, such as human

70   transketolase and periplasmic phosphate-binding proteins, to mediate ligand binding

71   and selectivity, implying LBHBs have the potential to be used for high selective drug

72   design [22, 23]. The intermolecular hydrogen bond between carboxylic acid and

73   pyridine was extensively studied and both experimental and theoretical calculation

74   evidences revealed this intermolecular hydrogen could be an LBHB [24-26]. Most

75   recently, an LBHB was found between pyrimidyl of thiamine and carboxyl of glu366

76   in human transketolase through ultra-high-resolution X-ray crystallography [22]. Thus,

77   it is possible that an LBHB could exist between inhibitors (containing pyridine or

78   pyridine-like function group) and its target protein and may have special biochemical

79   functions.

80   A synthetic compound, 3-(3-Phenoxybenzyl)amino-β-carboline (PAC, Fig 1a), belongs

81   to the class of known anti-cancer natural products [27] denoted β-carboline derivatives

82   [28-30]. PAC is a potent tubulin inhibitor with nanomolar IC_{50} values in several tumor

83   cells [30]. Tubulin is a validated target for a wide range of tumors and several drugs,

4

84   including paclitaxel, eribulin and vinca alkoloids, that inhibit the polymerization or

85   depolymerization of tubulin are in clinical use [31, 32]. We have determined that PAC

86   has a novel mode of action beyond simple inhibition of tubulin polymerization. We

87   show that PAC when given in relevant doses results in the specific degradation of

88   tubulin by the ubiquitin pathway. Our data indicate that ubiquitinylation is a response

89   to destabilization and aggregation of tubulin. Structural activity analysis reveals that an

90   LBHB between pyrimidyl of PAC and carboxyl of βGlu198 underpins the degradation.

91   While another two compounds forming normal hydrogen bonds with βGlu198

92   exhibited no tubulin degradation effect. We screened for other compounds that can form

93   LBHB with βGlu198 and identified that BML284, a Wnt signaling activator also

94   promoted tubulin heterodimers degradation in a PAC like manner.

95   Our study demonstrated a new role of LBHB in mediating protein stability by small

96   molecules, identified a novel approach to design tubulin degraders and suggest a new

97   strategy for drug development, designing small molecules to form LBHBs with protein

98   residues resulting in the highly specific degradation of a target protein. Also, the

99   interaction between the carboxylic acid and pyridine or pyridine-like function group

100   could be used as a model to design drugs forming LBHB with target protein.

101

102

5

103   *2.Results*

104   **2.1 PAC selectively downregulates the protein level of tubulin heterodimers**

105   PAC (Fig.1a) showed high anticancer activity *in vitro* [33], and is identified as a tubulin

106   inhibitor [30]. PAC induced obvious G2/M phase cell cycle arrest on human cervical

107   adenocarcinoma cell line HeLa and human colon colorectal carcinoma cell line Hct116

108   (**Fig.S1a**) and caspase-dependent apoptosis on HeLa cells (**Fig.S1b**). PAC significantly

109   and dose-dependently inhibited tumor growth of both human large cell lung carcinoma

110   cell line H460 and Hct116 xenografts (**Fig.S1c** and **S1d**). To illuminate the cellular

111   effect of PAC in an early time point, we employed a tandem mass tag (TMT)

112   quantitative proteomic analysis of six-hour PAC treated HeLa cells, and demonstrated

113   that PAC could specifically downregulate the protein level of α- and β-tubulin and their

114   subtypes (**Fig.1b**). The biological processes and cellular components analysis of the

115   quantitative proteomic data showed that the mitotic cell cycle was the most effected

116   biological process and cytoskeleton was the most effected cellular component in

117   response to PAC treatment (**Fig.S2a** and **S2b**). These results were consistent with

118   tubulin reduction since tubulin is the main component of cytoskeleton and plays an

119   important role in mitosis [34]. Immunoblot analysis similarly exhibited clear reduction

120   of α- and β-protein in HeLa, Hct116, H460 and human B cell lymphoma cell SU-DHL-

121   6 in a dose (**Fig.1c**) and time dependent manner for HeLa and Hct116 cells (**Fig 1d**). A

122   qPCR assay confirmed that the drop in level of αβ-tubulin proteins is post

123   transcriptional, since mRNA levels of αβ-tubulin in HeLa and Hct116 showed no such

124   time dependence (**Fig. S3a** and **S3b**). We also found PAC administration reduced the

125   protein level of tubulin in tumor tissue of an Hct116 xenograft model (**Fig.S3c**). *In vitro*

6

126   tubulin polymerization assay showed that PAC directly binds to purified tubulin and

127   inhibits tubulin polymerization in a concentration dependent manner (**Fig.S3d**). Of all

128   the widely known tubulin-binding agents we have tested, only PAC could induce the

129   degradation of tubulin (**Fig.1e**). To identify the binding site of PAC on tubulin and

130   whether the binding of PAC to tubulin accounts for the degradation effect, we carried

131   out competition assays and found that colchicine, but not vinblastine, maytansine or

132   pironetin inhibit PAC-induced tubulin degradation, suggesting that PAC exerts it effect

133   by binding to the colchicine site (**Fig.1f**). All these indicated PAC induces selective

134   tubulin degradation by binding to the colchicine site.

135   **2.2 PAC specifically destabilizes tubulin making it prone to aggregation that then**

136   **predisposes it to ubiquitinylation**

137   HeLa cells were pretreated with various inhibitors, including lysosome inhibitor

138   NH_4Cl, proteasome inhibitor MG132, autophagy inhibitor 3-MA. Only the proteasome

139   inhibitor MG132 completely blocked PAC-induced tubulin degradation (**Fig.2a** and

140   **S4a**), suggesting proteasome pathway is responsible for the tubulin degradation.

141   Immunoblot analysis of immunoprecipitated α- and β-tubulin by ubiquitin antibody

142   showed that PAC treatment has significantly increased the ubiquitinylation level of α-

143   and β-tubulin (**Fig.S4b**), whereas no such obvious effect on the general ubiquitinylation

144   level of the total proteins (**Fig.S4c**) was observed. PYR-41, a specific inhibitor for

145   ubiquitin-activating enzyme E1, completely inhibited PAC-induced tubulin degradation

146   (**Fig.2a**), suggesting PAC induced tubulin degradation relied on ubiquitinylation. Cells

147   pretreated with MG132 (or PYR-41) possessed aggregates of tubulin in cytoplasm after

7

148   PAC treatment (**Fig.2b**). Size-exclusion chromatography also revealed that PAC

149   treatment resulted in purified tubulin aggregation *in vitro* (**Fig.2c**), which was further

150   confirmed by transmission electron microscope (TEM) with lots of different size

151   spherical tubulin aggregates observed (**Fig.2d**). We speculated that PAC might promote

152   denaturation of tubulin and ubiquitinylation arise from normal protein clearance. Using

153   a Thiol Fluorescent Detection Kit the denaturation of both tubulin and bovine serum

154   albumin (BSA) were studied. While PAC showed no denaturation effect on BSA, it

155   promoted denaturation of tubulin at low concentrations, an effect that was inhibited by

156   pretreatment with colchicine (**Fig.2e**), confirming PAC induces selective denaturation

157   of tubulin *in vitro*. Differential scanning fluorimetry results indicated tubulin treated

158   with PAC showed obvious lower transition midpoint (Tm) whereas colchicine had no

159   effect (**Fig.2f**), demonstrating PAC decreases the stability of tubulin *in vitro*. We

160   conclude then that PAC specifically destabilizes tubulin making it prone to aggregation

161   that then predisposes it to ubiquitinylation.

162   **2.3 Crystal structure of tubulin-PAC complex**

163   Crystals of a protein complex composed of two αβ-tubulin heterodimers, the stathmin-

164   like protein RB3 and tubulin tyrosine ligase (T2R-TTL) [35] were soaked with PAC

165   and the resulting complex determined to 2.65 Å resolution (**Fig.3a**). Details of the data

166   collection and refinement statistics are summarized in **Supplementary Table 1**. The

167   Fo–Fc difference electron density identified there was a PAC molecule on each of β1-

168   tubulin and β2 tubulin (**Fig.3b**). Our previous structure-based pharmacophore for

169   colchicine binding site inhibitors (CBSIs) suggest there are five recognition centers:

8

170   three hydrophobic centers (I, II and III) and two hydrogen bond centers (IV and V) [36].

171   In this tubulin-PAC complex, PAC occupied hydrophobic centers I and II where it

172   makes extensive van der Waal contacts (**Fig.3c**). PAC forms hydrogen bonds with the

173   side chains of βE198 and βY200 in hydrogen bond center IV (**Fig.3c**). Compared to the

174   colchicine complex (PDB:4O2B) [37], PAC was located deeper in the β subunit and

175   made no interaction with α subunit consequently the atoms of PAC and colchicine show

176   only little overlap (**Fig.S5a**). Comparison between tubulin-PAC and tubulin-colchicine

177   complex structures showed that the binding did not affect the global conformation of

178   tubulin nor of the T2R complex. The root mean square deviation (RMSD) for 1,967 Cα

179   atoms between tubulin-PAC and tubulin-colchicine complexes is 0.4 Å.

180   **2.4 The pyridine nitrogen of PAC and Glu198 of β-tubulin mediate the tubulin**

181   **degradation.**

182   Informed by the crystal structure PAC-tubulin complex，we synthetized a series of PAC

183   derivatives to identify which functional group of PAC is responsible for its tubulin

184   degradation ability (**Fig.4a**). Compounds **9**, **10**, **11**, **14** and **15** showed anti-proliferation

185   and promoted tubulin degradation at higher concentrations (**Fig.4b, 4c** and **S5b**). For

186   ease of discussion, we decomposed PAC into three rings (**Fig.4a**). Since compound **9**

187   lacked the **C** ring of PAC, we conclude it is not essential. The activity of compounds

188   **10** and **11** exhibited that the **B** ring can be substituted by aliphatic ring or chain. The

189   binding mode of **9**– and **11**–tubulin complexes were similar to PAC (**Fig. S5c**).

190   Compounds **14** and **15** revealed that even the carboline ring (A ring) is not critical (**Fig**

191   **4d, 4e** and **S3b**). Compounds **20** and **24** were synthesized to probe the importance of

9

192   N-2 and -NH- group at C-3 position. Compound **20** lost both anti-proliferation and

193   tubulin degradation activity while compound **24** retained both (**Fig. 4b, 4c** and **S5b).**

194   We concluded that N-2 on the carboline ring is the key functional group contributing to

195   tubulin degradation. The crystal structure of PAC-tubulin complex demonstrated that

196   only βGlu198 and βTyr200 make polar interactions with N-2 of PAC. PAC addition

197   promoted wild-type like degradation of Y200F β-tubulins but had no effect on E198G,

198   E198Q or E198D β-tubulins (**Fig.4d**). EBI assay revealed that PAC no longer bound to

199   the colchicine site of β-tubulin mutants βE198G, βE198Q, or βE198D (**Fig.S5d**). We

200   concluded that the hydrogen bond interaction between βGlu198 and the nitrogen atom

201   at 2-position of A ring of PAC triggers tubulin degradation. However, two tubulin

202   inhibitors, nocodazole (Noc) and plinabulin (Pli), adopt similar conformations in β-

203   tubulin to PAC. and also form hydrogen bonds with βGlu198 (**Fig.4e**) [38], they could

204   not cause tubulin degradation effect and block PAC-induced degradation (**Fig.4f**),

205   suggesting that the hydrogen bond between OGlu198 and pyridine nitrogen of PAC

206   may be special.

207   **2.5 An LBHB between PAC and βGlu198 triggers tubulin degradation**

208   Several previous papers have identified the formation of LBHBs between carboxyl and

209   nitrogen of pyridyl in compounds complexes through chemical calculations, ultralow

210   temperature NMR and cocrystal structure studies [22, 24, 26, 38], which was almost

211   the same pattern with PAC-βGlu198 model. We calculated that the p*K*a value (using

212   Propka 3.1) of βGlu198 to be 9.6, indicating that it is neutral (protonated) under normal

213   conditions. Upon PAC binding, the p*K*a values of βGlu198 and pyridine nitrogen of

10

214   PAC in the PAC-crystal structure are 2.3 and 2.5 respectively, similar enough to indicate

215   the presence of an LBHB [39]. The interatomic distance between O_{Glu198} and

216   compounds in PAC-tubulin, Compound **9**-tubulin and Compound **11**-tubulin complex

217   is ranged from 2.66 to 2.83 Å (**Fig.5a**). Hydrogen bonds length in X-Ray crystal

218   structure is aligned longer than that in neutron crystal structure. For example, the length

219   of the Glu198-His198 LBHB in X-ray structure of sisomicin bound AAC-Via (6BC7)

220   is 2.84 Å, while in the neutron/X-ray structure (6BBZ) is 2.57 Å [20]. Thus, the length

221   of O_{Glu198}-N_{PAC} hydrogen bond could also meet the requirement of an LBHB. Besides,

222   in the QM/MM Optimized structure (more accurate than experimental structure for

223   reaction mechanism study [40-42]) the interatomic distance between O_{Glu198} and N_{PAC}

224   is 2.49 Å (**Fig.S6a**), which is far smaller than the sum of their van-der-Waals radii (2.65

225   Å for O-N pairs) and meets the need of an LBHB. Using QM/MM calculation, a mature

226   and widely used method for predicting LBHB [13, 22, 43-45], we found the potential

227   energy curve of O_{Glu198}-N_{PAC} hydrogen has a double-well character, and the computed

228   proton transfer barrier is 1.77 kcal/mol, which is well under the threshold that typically

229   indicates an LBHB and is under the sum of zero point vibrational energy (ZPVE, 1.46

230   kcal/mol) and kT (0.596 kcal/mol) (**Fig.5b**) [14]. Besides, QM/MM molecular

231   dynamics simulations clearly showed the proton is able to move freely between

232   βGlu198 and PAC (**Fig.5c-d, S6b-d**). In normal hydrogen bond, the splitting of

233   vibrational energy decreases as the vibration step rises (The $|1\rangle$ to $|2\rangle$ energy ε_{21} is

234   smaller than the $|0\rangle$ to $|1\rangle$ energy ε_{10}), while the PAC vibration energy splitting increases

235   with the rise of the vibration step ($\varepsilon_{21} > \varepsilon_{10}$) （**Table S2**）, resulting a superharmonicity

11

236   effect, which also suggested an LBHB [46]. In contrast, the potential energy curves and

237   vibration energy splitting decrease ($\varepsilon_{21} < \varepsilon_{10}$) of O_{Glu198}-N_{Noc} and O_{Glu198}-O_{Pli} indicate

238   these two tubulin inhibitors could not form LBHBs (**Fig.5b and Table S2**). All these

239   demonstrated that there is an LBHB formed between O_{Glu198} and N_{PAC} and the LBHB

240   is required for the tubulin degradation effect.

241   **2.6 Identification of a new tubulin degrader with the LBHB mediated degradation**

242   **mechanism**

243   To further confirm of the degradation mechanism and identify effective new tubulin

244   degradation compounds, we screened compounds from lots of tubulin inhibitors with

245   molecular docking and QM/MM calculation and found BML284 (**Fig.6a**), a Wnt

246   signaling activator and tubulin inhibitor [47], might form an LBHB with βGlu198.

247   Crystal structure of tubulin-BML284 complex validated that BML284 binds to

248   colchicine site and forms a hydrogen bond with βGlu198 (**Fig.6b and S7a**), which was

249   proved to be an LBHB by QM/MM calculation as validated by a symmetric double well

250   and low barrier potential energy curve and vibration energy splitting increase ($\varepsilon_{21} > \varepsilon_{10}$)

251   (**Fig.6c and Table S2**). Superimposition of the tubulin–BML284 structure onto that of

252   tubulin–PAC showed these two compounds overlap and both form an LBHB with

253   βGlu198 in a similar manner (**Fig.S7b**). Immunoblotting results revealed BML284

254   indeed promotes tubulin heterodimers protein degradation in a concentration dependent

255   manner while exhibits no effect on their mRNA levels (**Fig.6d and S7c**). The same as

256   PAC, BML284-induced tubulin degradation could also be blocked by colchicine or

257   PYR-41 (**Fig.6e and 6f**). TEM results confirmed that BML284 also induces spherical

258   tubulin aggregates formation *in vitro* (**Fig.6g**). Thiol Fluorescent Detection Kit Assay

259   also indicated that BML284 induces purified tubulin denaturation (**Fig.6h**).Taken

260   together, we identified a new tubulin degrader using the LBHB mediated degradation

261   mechanism.

262   **3. Discussion**

263   The human cell flags proteins for degradation by ubiquitinylation either through

264   specific events (for example MDM2) [48] or as normal housekeeping to remove

265   misfolded or denatured proteins [49]. Proteins with reduced stability are prone to

266   unfolding and therefore more efficiently cleared in the normal housekeeping [50].

267   Molecules which promote protein ubiquitinylation will lead to proteolytic degradation

268   of the targeted proteins are well established medicines [51].

269   Our data indicate there is a new method of specifically promoting target protein

270   degradation. PAC, a known tubulin inhibitor [30], effectively destabilizes tubulin and

271   thereby promotes its degradation as part of normal cell housekeeping. This effect is

272   very specific since no widespread protein destabilization was observed and the effect is

273   distinct from compounds such as isothiocyanates or withaferin A that also promote

274   tubulin degradation. These compounds non-specifically bind to free protein thiols and

275   promote degradation and / or alter the function of many proteins (isothiocyanates: Nrf,

276   CDC25, GSH, MIF, STAT3 *et al* [52] and withaferin A: vimentin, actin HSP90, annexin

277   II *et al* [53-55]), not just tubulin [56, 57].

278   Interestingly the co-complex of PAC with tubulin does not reveal any significant

279   conformational changes that could easily explain the effect. However, structure-

13

280   activity-relationship analysis using variants of PAC and site directed mutagenesis of β-

281   tubulin, identifies a single key interaction, that between the pyridine nitrogen of PAC

282   and βGlu198 (interior hydrophobic region of β-tubulin) as the trigger for degradation.

283   Detailed calculations study show these two groups form an LBHB whilst other

284   inhibitors, Noc and Pli, form only normal hydrogen bonds with βGlu198 and do not

285   destabilize tubulin. We conclude that it is the LBHB between PAC and tubulin that

286   destabilizes tubulin and consequently the protein is prone to unfolding and clearance

287   via the house keeping ubiquitin system. The deep mechanism of LBHB mediate tubulin

288   destabilization remains further investigation and here we proposed two possible

289   hypothesizes: LBHB has unusual strong strength with some extent covalent character

290   [46, 58], thus its abnormally strong strength could help to trap an unstable conformation

291   of tubulin; Formation of an LBHB will release 10-20 kcal/mol energy and also the

292   significant decrease in pKa of βGlu198（from 9.6 to 2.3）will release about 10 kcal/mol

293   energy as calculated by delta G^o = 2.303RT(delta pKa) [9, 59]. Therefore, a total 20-30

294   kcal/mol energy could make unfold of tubulin owing to the associated loss of net

295   stability [60].

296   Using this LBHB mediated degradation mechanism we screened for compounds from

297   lots of tubulin inhibitors with QM/MM calculation and molecular docking methods and

298   found BML284, a Wnt signaling activator and tubulin inhibitor, can also form an LBHB

299   with βGlu198 and promote tubulin degradation in a PAC-like manner as expected.

300   Since LBHB was firstly proposed in the early 1990s, there have been few reports on

301   other biochemical effects besides its roles in participating in enzyme catalysis and

302   maintain protein structural integrity [10, 21, 22]. Our study confirms a new role of

303   LBHB in mediating protein stability by small molecules, which could be utilized for

304   novel drug discovery.

305   Molecules which form LBHB with buried residues represent a powerful new strategy

306   in medicinal chemistry. These molecules are very different from the chaotropic agents

307   that denature most proteins, they rely on specific protein ligand interactions. In another

308   advantage, they are smaller and more "drug" like than the large proteolysis targeting

309   chimaeras type molecules. The geometric constraints of the LBHB impose a high

310   degree of selectivity upon those molecules thus reducing, at least in theory, unwanted

311   side effects. As we have shown there exist excellent tools to judge whether any

312   molecule participates in such an LBHB with a protein and measurement of the effect of

313   such an LBHB upon protein stability is straightforward. These factors mean such an

314   approach could be widely adopted.

315   **Acknowledgements**

322   **Author contributions**

323   J.Y. performed most of the cellular and biochemical experiments and wrote the draft.

15

324   Y.L. synthesized all chemical compounds. Q.Q. performed the tubulin mutation and

325   animal experiments. R.W. and D.X. performed the computational calculations. W.Y,

326   Y.Y, L.N., and Q.C. performed the structural biology experiments. H.P., H.W., L.O.

327   and H.Y. analyzed the data. J.Y., Q.C., W.L. and L.C. conceived the idea and

328   supervised the study. Q.C., and L.C. revised the manuscript.

329   All authors approved the final manuscript.

330   **Competing interests**

331   The authors declare no competing financial interests.

332   **Correspondence and requests for materials** should be addressed to Q.C. or L.C.

333   **Data availability.**

334   Atomic coordinates and structure factors of tubulin complexed with PAC, Compound

335   9, Compound 11 or BML284 have been deposited in the Protein Data Bank under

336   accession codes 7CDA, 7CE6, 7CE8 and 7CEK, respectively. All other data are

337   available from the corresponding authors on reasonable request.

338

339   **Reference**

340   [1] Minch MJ. An introduction to hydrogen bonding (Jeffrey, George A.). ACS Publications; 1999.

341   [2] Hibbert F, Emsley J. Hydrogen bonding and chemical reactivity.   Advances in physical organic

342   chemistry: Elsevier; 1990. p. 255-379.

343   [3] Perrin CL, Nielson JB. "Strong" hydrogen bonds in chemistry and biology. Annual review of physical

344   chemistry. 1997;48:511-44.

345   [4] Grabowski SJ. Hydrogen bonding: new insights: Springer; 2006.

346   [5] Enciso M, Rey A. Improvement of structure-based potentials for protein folding by native and

347   nonnative hydrogen bonds. Biophysical journal. 2011;101:1474-82.

348   [6] Bordo D, Argos P. The role of side-chain hydrogen bonds in the formation and stabilization of

349   secondary structure in soluble proteins. Journal of molecular biology. 1994;243:504-19.

350   [7] Shan S-o, Herschlag D. [11] Hydrogen bonding in enzymatic catalysis: Analysis of energetic

351   contributions.   Methods in enzymology: Elsevier; 1999. p. 246-76.

352   [8] Cleland W. Low-barrier hydrogen bonds and low fractionation factor bases in enzymic reactions.

353   Biochemistry. 1992;31:317-9.

354   [9] Cleland W, Kreevoy MM. Low-barrier hydrogen bonds and enzymic catalysis. Science.
355   1994;264:1887-90.

356   [10] Cleland W. Low-barrier hydrogen bonds and enzymatic catalysis. Archives of Biochemistry and
357   Biophysics. 2000;382:1-5.

358   [11] Cleland WW. Low-Barrier Hydrogen Bonds and Enzymatic Catalysis ☆. Science. 1994;264:1887-
359   90.

360   [12] Nichols DA, Hargis JC, Sanishvili R, Jaishankar P, Defrees K, Smith EW, et al. Ligand-Induced
361   Proton Transfer and Low-Barrier Hydrogen Bond Revealed by X-ray Crystallography. Journal of the
362   American Chemical Society. 2015;137:8086.

363   [13] Hosur M, Chitra R, Hegde S, Choudhury R, Das A, Hosur R. Low-barrier hydrogen bonds in proteins.
364   Crystallography reviews. 2013;19:3-50.

365   [14] Nichols DA, Hargis JC, Sanishvili R, Jaishankar P, Defrees K, Smith EW, et al. Ligand-induced
366   proton transfer and low-barrier hydrogen bond revealed by X-ray crystallography. Journal of the
367   American Chemical Society. 2015;137:8086-95.

368   [15] Saito K, Ishikita H. Formation of an unusually short hydrogen bond in photoactive yellow protein.
369   Biochimica et Biophysica Acta (BBA)-Bioenergetics. 2013;1827:387-94.

370   [16] Gu Z, Drueckhammer DG, Kurz L, Liu K, Martin DP, McDermott A. Solid state NMR studies of
371   hydrogen bonding in a citrate synthase inhibitor complex. Biochemistry. 1999;38:8022-31.

372   [17] Markley JL, Westler WM. Protonation-state dependence of hydrogen bond strengths and exchange
373   rates in a serine protease catalytic triad: bovine chymotrypsinogen A. Biochemistry. 1996;35:11092-7.

374   [18] Zhao Q, Abeygunawardana C, Gittis AG, Mildvan AS. Hydrogen bonding at the active site of Δ5-
375   3-ketosteroid isomerase. Biochemistry. 1997;36:14616-26.

376   [19] Dajnowicz S, Parks JM, Hu X, Gesler K, Kovalevsky AY, Mueser TC. Direct evidence that an
377   extended hydrogen-bonding network influences activation of pyridoxal 5′-phosphate in aspartate
378   aminotransferase. Journal of Biological Chemistry. 2017;292:5970-80.

379   [20] Kumar P, Serpersu EH, Cuneo MJ. A low-barrier hydrogen bond mediates antibiotic resistance in a
380   noncanonical catalytic triad. Science advances. 2018;4:eaas8667.

381   [21] Langkilde A, Kristensen SM, Lo Leggio L, Mølgaard A, Jensen JH, Houk AR, et al. Short strong
382   hydrogen bonds in proteins: a case study of rhamnogalacturonan acetylesterase. Acta Crystallographica
383   Section D: Biological Crystallography. 2008;64:851-63.

384   [22] Dai S, Funk L-M, von Pappenheim FR, Sautner V, Paulikat M, Schröder B, et al. Low-barrier
385   hydrogen bonds in enzyme cooperativity. Nature. 2019;573:609-13.

386   [23] Elias M, Wellner A, Goldin-Azulay K, Chabriere E, Vorholt JA, Erb TJ, et al. The molecular basis
387   of phosphate discrimination in arsenate-rich environments. Nature. 2012;491:134-7.

388   [24] Perrin C. Low-barrier hydrogen bonds in pyridine-dichloroacetic acid complexes. Polish Journal of
389   Chemistry. 2003;77:1693-702.

390   [25] Golubev NS, Smirnov SN, Tolstoy PM, Sharif S, Toney MD, Denisov GS, et al. Observation by
391   NMR of the tautomerism of an intramolecular OHOHN-charge relay chain in a model Schiff base.
392   Journal of Molecular Structure. 2007;844:319-27.

393   [26] Koeppe B, Pylaeva S, Allolio C, Sebastiani D, Nibbering E, Denisov G, et al. Polar solvent
394   fluctuations drive proton transfer in hydrogen bonded complexes of carboxylic acid with pyridines: NMR,
395   IR and ab initio MD study. Physical Chemistry Chemical Physics. 2017;19:1010-28.

396   [27] Haarmann ST, Sendker JC, Krug N, Bothe H, Fritsche E, Proksch P, et al. Regulation of dioxin

17

397   receptor function by different beta-carboline alkaloids. Archives of Toxicology. 2010;84:619-29.

398   [28] Wu Q, Bai Z, Ma Q, Fan W, Guo L, Zhang G, et al. Synthesis and biological evaluation of novel
399   bivalent β-carbolines as potential antitumor agents. Medchemcommun. 2014;5:953-7.

400   [29] Zhang M, Sun D. Recent Advances of Natural and Synthetic β-Carbolines as Anticancer Agents.
401   Anti-Cancer Agents in Medicinal Chemistry (Formerly Current Medicinal Chemistry - Anti-Cancer
402   Agents). 2015;15:-.

403   [30] Ikeda R, Kurosawa M, Okabayashi T, Takei A, Yoshiwara M, Kumakura T, et al. 3-(3-
404   Phenoxybenzyl)amino-β-carboline: a novel antitumor drug targeting α-tubulin. Bioorganic & Medicinal
405   Chemistry Letters. 2011;21:4784.

406   [31] Yang J, Li Y, Yan W, Li W, Qiu Q, Ye H, et al. Covalent modification of Cys-239 in β-tubulin by
407   small molecules as a strategy to promote tubulin heterodimer degradation. Journal of Biological
408   Chemistry. 2019;294:8161-70.

409   [32] Yang J, Wang Y, Wang T, Jiang J, Botting CH, Liu H, et al. Pironetin reacts covalently with cysteine-
410   316 of α-tubulin to destabilize microtubule. Nature Communications. 2016;7:12103.

411   [33] Ikeda R, Kurosawa M, Okabayashi T, Takei A, Yoshiwara M, Kumakura T, et al. 3-(3-
412   Phenoxybenzyl)amino-beta-carboline: A novel antitumor drug targeting alpha-tubulin. Bioorg Med
413   Chem Lett. 2011;21:4784-7.

414   [34] Fenderson, Bruce. Molecular Biology of the Cell,5th Edition. Shock. 2008;30.

415   [35] Prota AE, Bargsten K, Zurwerra D, Field JJ, Díaz JF, Altmann KH, et al. Molecular mechanism of
416   action of microtubule-stabilizing anticancer agents. Science. 2013;339:587-90.

417   [36] Wang Y, Zhang H, Gigant B, Yu Y, Wu Y, Chen X, et al. Structures of a diverse set of colchicine
418   binding site inhibitors in complex with tubulin provide a rationale for drug discovery. Febs Journal.
419   2016;283:102-11.

420   [37] Prota AE, Franck D, Felix B, Katja B, Buey RM, Jens P, et al. The novel microtubule-destabilizing
421   drug BAL27862 binds to the colchicine site of tubulin with distinct effects on microtubule organization.
422   Journal of Molecular Biology. 2014;426:1848-60.

423   [38] Bedekovi N, Stili V, Pit T. Aromatic versus Aliphatic Carboxyl Group as a Hydrogen Bond
424   Donor in Salts and Cocrystals of an Asymmetric Diacid and Pyridine Derivatives. Crystal Growth &
425   Design. 2017;17:5732-43.

426   [39] Gilli G, Gilli P. Towards an unified hydrogen-bond theory. Journal of Molecular Structure.
427   2000;552:1-15.

428   [40] Fu Z, Li X, Merz Jr KM. Accurate assessment of the strain energy in a protein‐bound drug using
429   QM/MM X‐ray refinement and converged quantum chemistry. Journal of computational chemistry.
430   2011;32:2587-97.

431   [41] Wu S, Xu D, Guo H. QM/MM Studies of Monozinc-Lactamase CphA Suggest That the Crystal
432   Structure of an Enzyme-Intermediate Complex Represents a Minor Pathway.

433   [42] Li X, Hayik SA, Merz Jr KM. QM/MM X-ray refinement of zinc metalloenzymes. Journal of
434   inorganic biochemistry. 2010;104:512-22.

435   [43] Mulholland AJ, Lyne PD, Karplus M. Ab initio QM/MM study of the citrate synthase mechanism.
436   A low-barrier hydrogen bond is not involved. Journal of the American Chemical Society. 2000;122:534-
437   5.

438   [44] Porter MA, Molina PA. The Low-Barrier Double-Well Potential of the Oδ1− H− Oδ1 Hydrogen
439   Bond in Unbound HIV Protease: A QM/MM Characterization. Journal of chemical theory and
440   computation. 2006;2:1675-84.

441 [45] Schutz CN, Warshel A. The low barrier hydrogen bond (LBHB) proposal revisited: The case of the
442 Asp··· His pair in serine proteases. Proteins: Structure, Function, and Bioinformatics. 2004;55:711-23.

443 [46] Dereka B, Yu Q, Lewis NH, Carpenter WB, Bowman JM, Tokmakoff A. Crossover from hydrogen
444 to chemical bonding. Science. 2021;371:160-4.

445 [47] Fukuda Y, Sano O, Kazetani K, Yamamoto K, Iwata H, Matsui J. Tubulin is a molecular target of
446 the Wnt-activating chemical probe. BMC biochemistry. 2016;17:9.

447 [48] Marine J-C, Lozano G. Mdm2-mediated ubiquitylation: p53 and beyond. Cell Death &
448 Differentiation. 2010;17:93-102.

449 [49] Goldberg AL. Protein degradation and protection against misfolded or damaged proteins. Nature.
450 2003;426:895-9.

451 [50] Schrader EK, Harstad KG, Matouschek A. Targeting proteins for degradation. Nature Chemical
452 Biology. 2009;5:815-22.

453 [51] Lai AC, Crews CM. Induced protein degradation: an emerging drug discovery paradigm. Nature
454 Reviews Drug Discovery. 2017;16:101-14.

455 [52] Mi L, Pasqua AJD, Chung FL. Proteins as binding targets of isothiocyanates in cancer prevention.
456 Carcinogenesis. 2011;32:1405.

457 [53] Bargagnamohan P, Hamza A, Kim YE, Khuan AHY, Morvaknin N, Wendschlag N, et al. The tumor
458 inhibitor and antiangiogenic agent withaferin A targets the intermediate filament protein vimentin.
459 Chemistry & Biology. 2007;14:623-34.

460 [54] Falsey RR, Marron MT, Gunaherath GMKB, Shirahatti N, Mahadevan D, Gunatilaka AAL, et al.
461 Actin microfilament aggregation induced by withaferin A is mediated by annexin II. Nature Chemical
462 Biology. 2006;2:33.

463 [55] Yu Y, Hamza A, Zhang T, Gu M, Zou P, Newman B, et al. Withaferin A targets heat shock protein
464 90 in pancreatic cancer cells. Biochemical Pharmacology. 2010;79:542.

465 [56] Geng F, Tang L, Li Y, Yang L, Choi KS, Kazim AL, et al. Allyl Isothiocyanate Arrests Cancer Cells
466 in Mitosis, and Mitotic Arrest in Turn Leads to Apoptosis via Bcl-2 Protein Phosphorylation. Journal of
467 Biological Chemistry. 2011;286:32259.

468 [57] Antony ML, Lee J, Hahm ER, Kim SH, Marcus AI, Kumari V, et al. Growth arrest by the antitumor
469 steroidal lactone withaferin A in human breast cancer cells is associated with down-regulation and
470 covalent binding at cysteine 303 of β-tubulin. Journal of Biological Chemistry. 2014;289:1852.

471 [58] Tolborg K, Jørgensen MR, Sist M, Mamakhel A, Overgaard J, Iversen BB. Low‐Barrier Hydrogen
472 Bonds in Negative Thermal Expansion Material H3 [Co (CN) 6]. Chemistry–A European Journal.
473 2019;25:6814-22.

474 [59] Fitch CA, Platzer G, Okon M, Garcia‐Moreno E B, McIntosh LP. Arginine: Its pKa value revisited.
475 Protein science. 2015;24:752-61.

476 [60] Dwyer JJ, Gittis AG, Karp DA, Lattman EE, Spencer DS, Stites WE. High apparent dielectric
477 constants in the interior of a protein reflect water penetration. Biophysical journal. 2000;79:1610-20.

478

479 **Table S1. Data collection and refinement statistics.**

	PAC	Compound 9	Compound 11	BML284
Data collection				
Space group	$P2_12_12_1$	$P2_12_12_1$	$P2_12_12_1$	$P2_12_12_1$

Cell dimensions				
a, b, c (Å)	77.9 78.0 177.6	105.3 157.5 182.4	105.3 157.7 181.5	105.6 158.1 181.3
α, β, γ (°)	90.0 90.0 90.0	90.0 90.0 90.0	90.0 90.0 90.0	90.0 90.0 90.0
Resolution (Å)	40.0-2.65 (2.71-2.65) *	50.0-2.70 (2.76-2.70) *	50.0-2.73 (2.79-2.73) *	119.2-2.70(2.86-2.70)
R_{pim}	4.9 (40.3)	6 (46.7)	7.5 (33.3)	7.3(59.3)
$I/\sigma I$	16.3 (2.1)	12.9 (2.0)	10.2 (2.3)	14.5(1.4)
Completeness (%)	99.9 (99.4)	100 (100)	100 (100)	99.8(64.6)
Redundancy	7.1 (6.8)	6.7(6.4)	6.7 (6.8)	10.9(10.5)
Refinement				
Resolution (Å)	39.8-2.66	47.0-2.70	48.1-2.73	48.3-2.70
No. reflections	85,700	82,400	79,992	83978
R_{work}/ R_{free}	22.2/25.7	22.4/24.9	20.7/ 24.2	22.8/27.1
No. atoms				
Protein	17413	17273	17903	17458
Ligand/ion	235	215	227	231
Water	381	351	272	13
B-factors				
Protein	41	42	45	65
Ligand/ion	47	44	46	72
Water	43	45	43	41
R.m.s deviations				
Bond lengths (Å)	0.003	0.004	0.003	0.006
Bond angles (º)	0.661	0.800	0.698	0.767

480   *Highest resolution shell is shown in parenthesis.

481

20

482 **Table S2**. Vibrational energy levels (ε in kcal/mol) for the first three states of
483 the proton in hydrogen bond between βGlu198 and compounds.

	State	ε	$\triangle \varepsilon$	
PAC	0	1.46		
	1	2.63	$\varepsilon_{10} = \varepsilon_{State\,1} - \varepsilon_{State\,0} = 1.17$	$\varepsilon_{10} < \varepsilon_{21}$
	2	3.90	$\varepsilon_{21} = \varepsilon_{State\,2} - \varepsilon_{State\,1} = 1.27$	
Noc	0	1.87		
	1	3.85	$\varepsilon_{10} = \varepsilon_{State\,1} - \varepsilon_{State\,0} = 1.98$	$\varepsilon_{10} > \varepsilon_{21}$
	2	4.87	$\varepsilon_{21} = \varepsilon_{State\,2} - \varepsilon_{State\,1} = 1.02$	
Pli	0	3.20		
	1	8.06	$\varepsilon_{10} = \varepsilon_{State\,1} - \varepsilon_{State\,0} = 4.86$	$\varepsilon_{10} > \varepsilon_{21}$
	2	11.67	$\varepsilon_{21} = \varepsilon_{State\,2} - \varepsilon_{State\,1} = 3.61$	
BML284	0	1.33		
	1	2.34	$\varepsilon_{10} = \varepsilon_{State\,1} - \varepsilon_{State\,0} = 1.01$	$\varepsilon_{10} < \varepsilon_{21}$
	2	3.82	$\varepsilon_{21} = \varepsilon_{State\,2} - \varepsilon_{State\,1} = 1.48$	

484

Figure 1
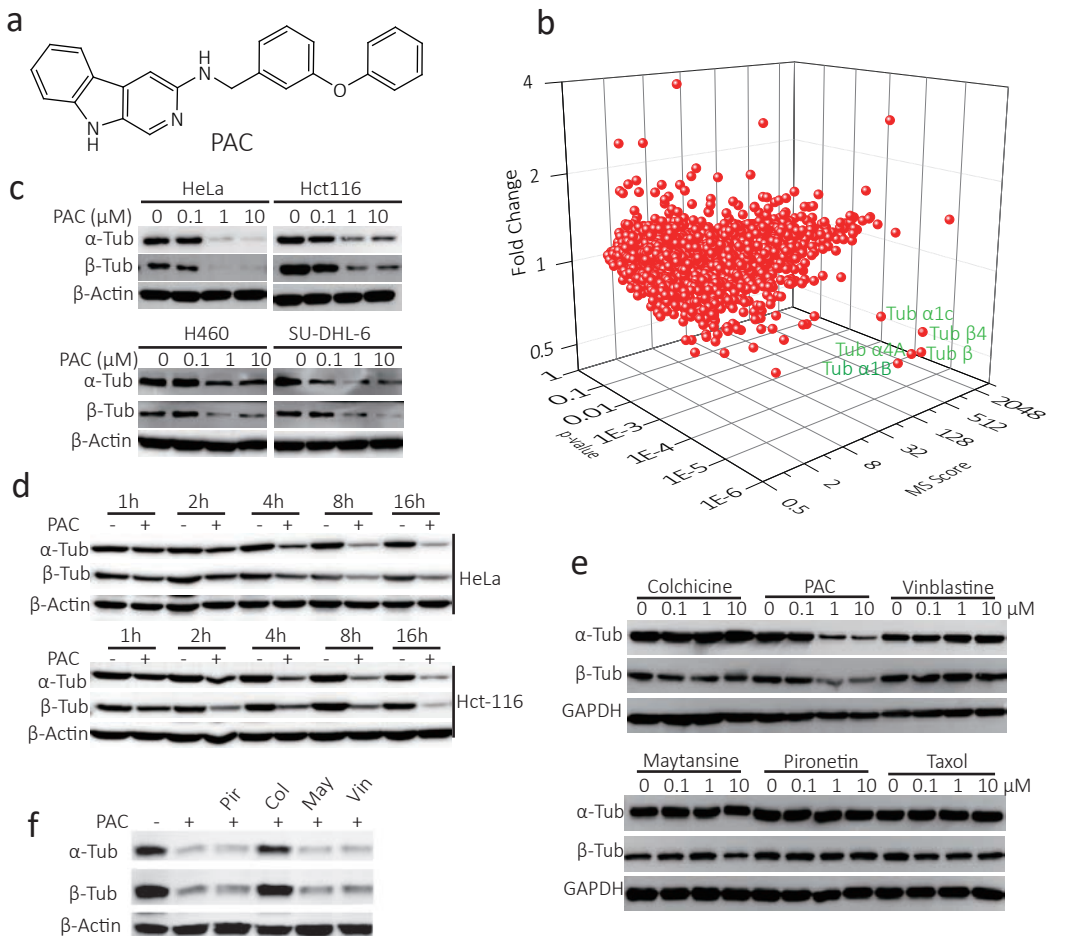
Figure 1: PAC selectively downregulates the protein level of αβ-tubulin heterodimers. (**a**) Chemical structure of PAC. (**b**) Proteome-wide analysis of HeLa cells treated with 1 μM PAC or DMSO alone for 6 hours using tandem mass tag quantitative proteomics. Each point represents the ratio of mean protein levels of three biological repetition in PAC- versus DMSO-treated cells. (**c**) Immunoblot analysis of α- and β-tubulin protein levels in HeLa, Hct116, H460 and SU-DHL-6 cells treated with the indicated concentrations of PAC for 24 h. β-Actin was used as loading control. Results are representative of three independent experiments. (**d**) Time course of α- and β-tubulin protein levels in HeLa and Hct116 cells treated with 1 μM PAC or DMSO. β-Actin was used as the loading control. Immunoblot results are representative of three independent experiments. (**e**) Comparing the tubulin degradation effect of PAC with conventional tubulin inhibitors. HeLa cells were treated with different concentrations of PAC, colchicine, vinblastine, maytansine, pironetin and taxol for 16hours, then α- and β-tubulin protein levels were detected by immunoblot. Results are representative of two independent experiments. (**f**) Inhibition of αβ-tubulin heterodimers degradation by tubulin inhibitors. HeLa cells were treated with or without 1μM pironetin，colchicine，maytansine and vinblastine for 1hour before treated with or without 1μM PAC for 16hours. Then cell α- and β-tubulin protein levels were monitored by immunoblot analysis. Results are representative of three independent experiments.

Figure 2
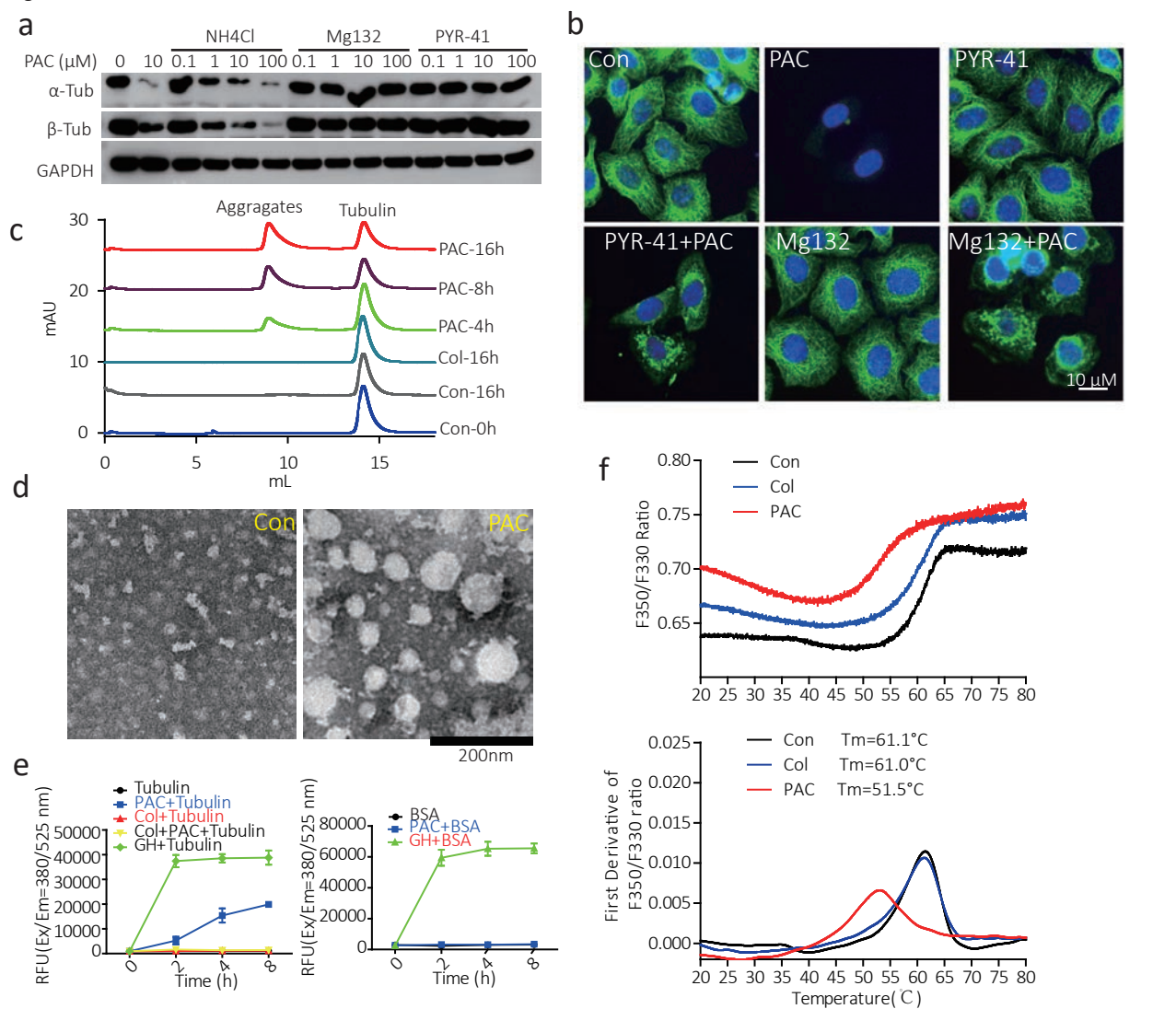
Figure 2: PAC promotes tubulin destabilization and aggregation. (**a**) Proteasome and ubiquitin inhibitors rescue PAC-induced tubulin degradation. HeLa cells were pretreated with 20 mM NH4Cl, 20 μM Mg132 or 20 μM PYR-41 for one hour before the addition of PAC. Results are representative of three independent experiments. (**b**) PAC induced tubulin aggregation in cytoplasm. HeLa cells were pretreated with Mg132 or PYR-41 for 1 hours before treated with PAC for 4 hours. The tubulin morphology was monitored by immunofluorescence. Results are representative of three independent experiments. (**c**) Gel filtration assays detection of tubulin aggregation. Purified tubulin was dissolved to 3μM in PEM buffer at room temperature before incubated with different compounds for different times. After incubation, samples were analyzed by a gel filtration assay. Results are representative of two independent experiments. (**d**) Transmission electron microscopy (TEM) detection of tubulin. Purified tubulin (10 μM) was incubated with or without 20μM PAC for 4 hours at room temperature, the images were taken by TEM. Results are representative of two independent experiments. (**e**) PAC promotes purified tubulin denaturation. Tubulin (1μM) was incubated with guanidine hydrochloride（GH）or other compounds or DMSO for 2, 4 or 8hours at room temperature. Then master reaction mix was added to the samples and incubated for another 30min. At last the fluorescent adduct were detected by a Biotech Gen5 spectrophotometer (λex = 380/λem = 525 nm). Data are shown as the mean ± SD (n = 3). (**f**) Thermal unfolding curves of DMSO, PAC (30 μM) or colchicine (30 μM) treated purified tubulin（3 μM）by a differential scanning fluorimetry (DSF) method. Plots of the fuorescence F350/F330 ratio (up) and the first derivative of F350/F330 ratio (low) are shown. Results are representative of three independent experiments.

Figure 3
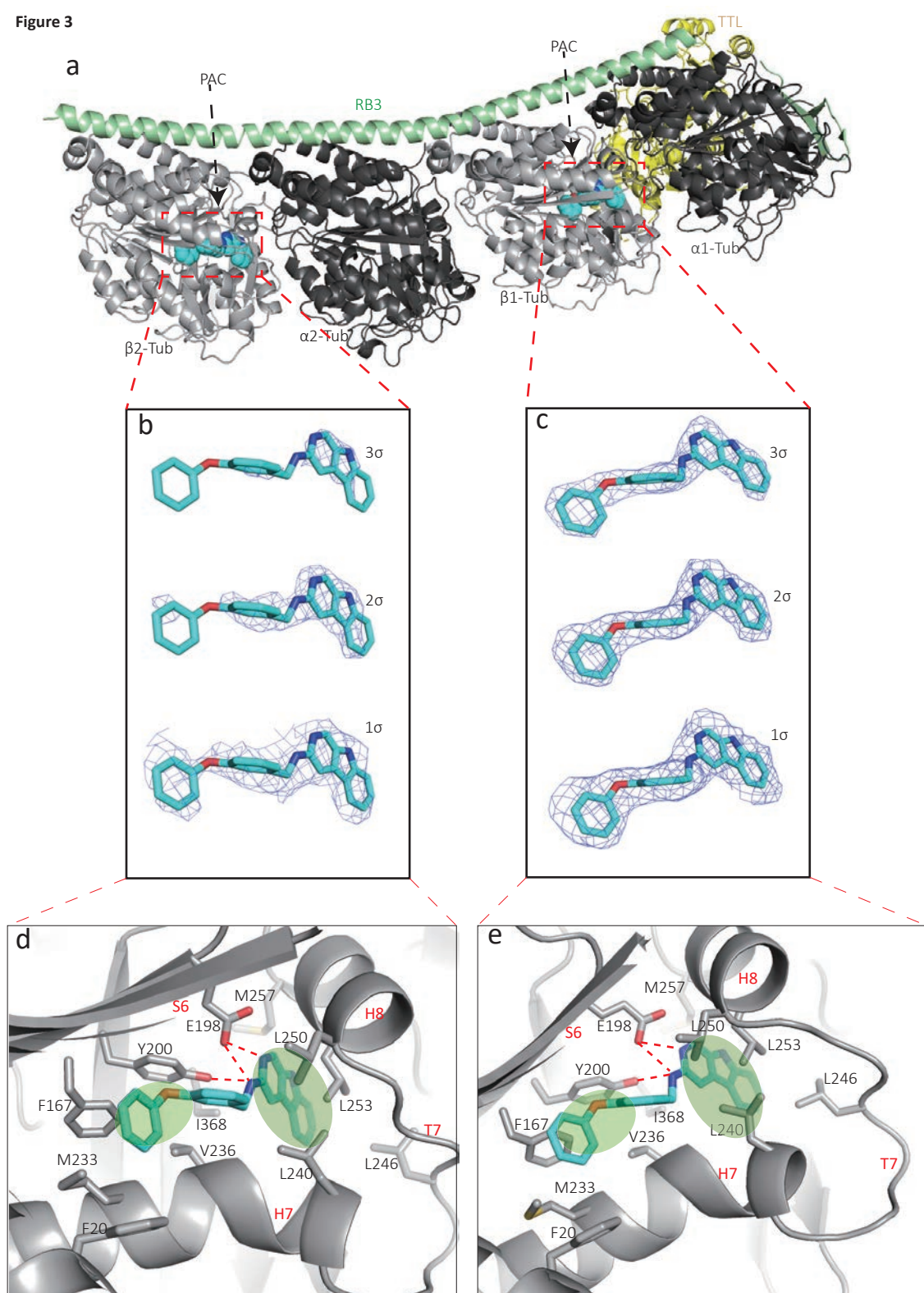
Figure 3: Crystal structure of PAC-tubulin complex. (a) Overall structure of tubulin-PAC complex. The RB3-SLD is colored green, TTL is yellow, α-tubulin is black, β-tubulin is grey, and PAC is cyan. PAC is shown as spheres. (b, c) Electron densities of PAC on (b) β2-tubulin or (c) β1-tubulin. The Fo-Fc omit map is colored light blue and contoured at 3δ, 2δ and 1δ. (d, e) Interactions between PAC and (d) β2-tubulin and (e) β1-tubulin. Residues that make interactions with PAC are shown as sticks and are labeled. The hydrophobic centers are indicated by green semitransparent ovals (small: center I; big: center II). Hydrogen bonds are drawn with red dashed lines.

Figure 4
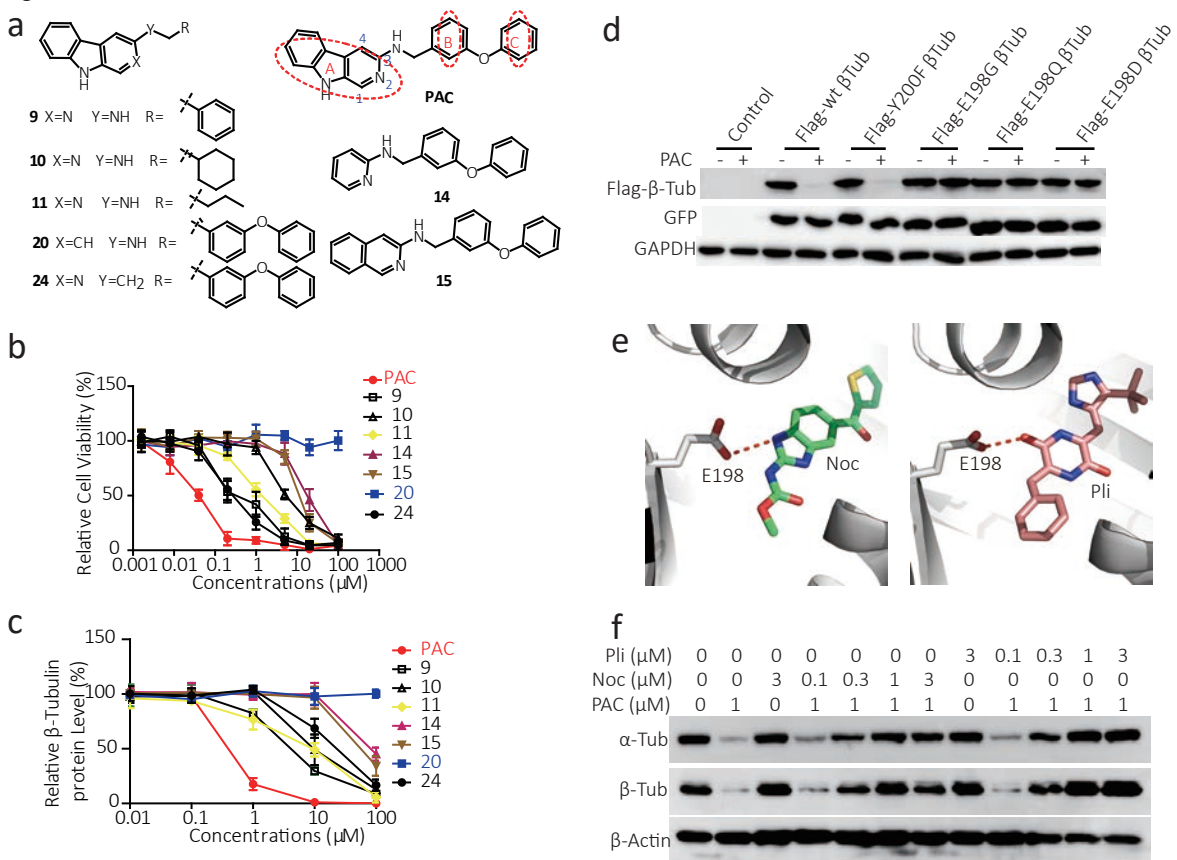
Figure 4: The pyridine nitrogen of PAC and Glu198 of β-tubulin mediate the tubulin degradation. (**a**) Chemical structure of synthetic PAC derivatives. (**b**) Growth inhibitory curves of PAC derivatives in HeLa cells. Cells were treated with different concentrations of indicated compound for 48 hours, cell viability were monitored by MTT assay. Data are shown as the mean ± SD (n = 3). (**c**) Tubulin degradation activity of PAC derivatives. HeLa cells were treated with different concentrations of indicated compound for 16hours, the tubulin protein levels were monitored by immunoblot. Densitometric quantification of immunoblot was performed by Image Quant TL software, Data are shown as the mean ± SD (n = 3). (**d**) Effect of PAC on tubulin mutants. MSCV-IRES-GFP vectors expressing both GFP and wild type or mutant Flag-β-tubulin were transfected to HeLa cells. After 24 hours, cells were treated with or without PAC for 16hours. Then the protein level of Flag-tubulin and GFP were detected by immunoblot. GAPDH were used as loading control. Results are representative of three independent experiments. (**e**) Close-up views of the interaction between βGlu198 with nocodazole (Noc) and plinabulin (Pli). (**f**) Inhibition of tubulin heterodimers degradation by colchicine site tubulin inhibitors. Hela cells were treated with different concentrations nocodazole and plinabulin for one hour before addition of PAC. Results are representative of two independent experiments.

Figure 5
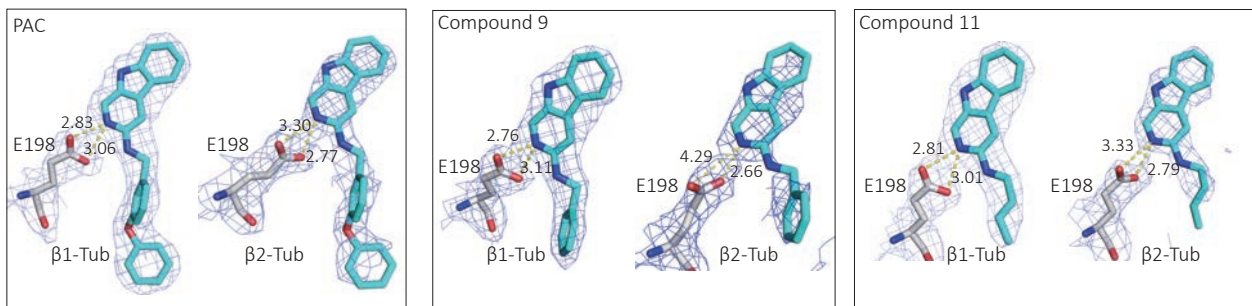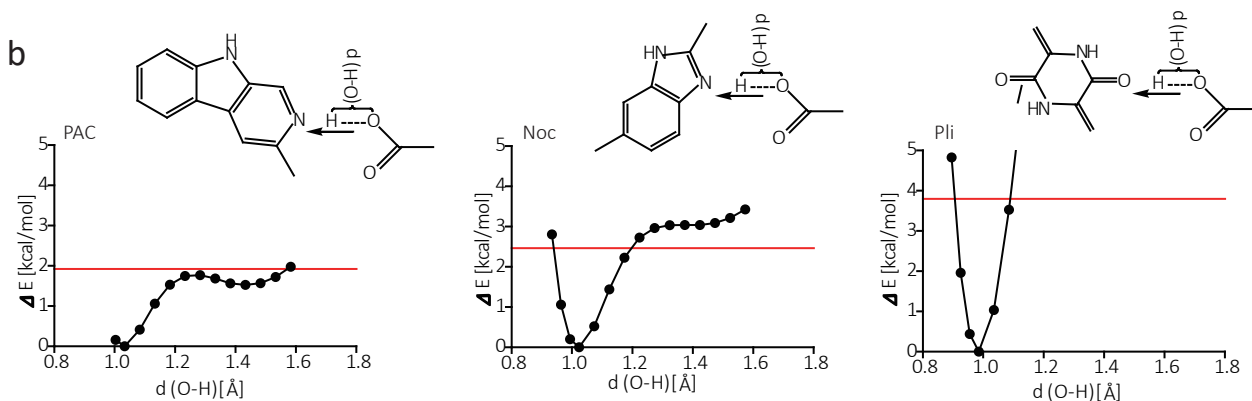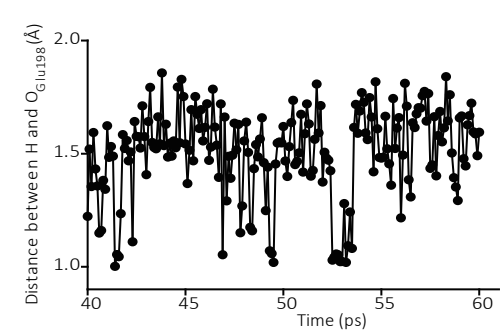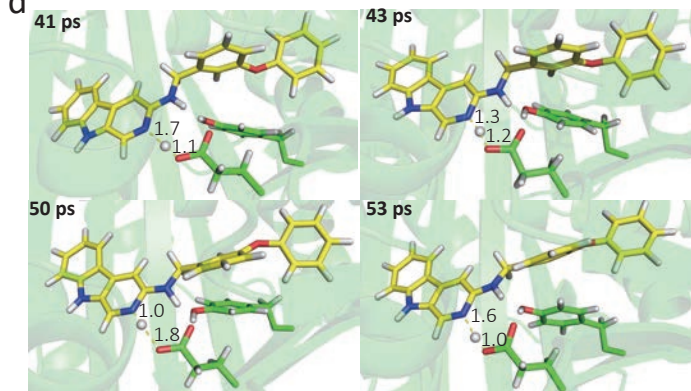
Figure 5: An LBHB between PAC and βGlu198 mediates tubulin degradation. (a) Distance between nitrogen of compounds (PAC, compound 9 and compound 11) to βGlu198. The 2Fo-Fc omit map is colored light blue and contoured at 1δ. Compounds and βGlu198 is shown in sticks and colored in cyan and grey respectively. (b) Energy profiles along the proton transfer coordinate for H-bond donor-acceptor pairs of the OGlu198-NPAC, OGlu198-NNoc and OGlu198-OPli hydrogen bonds. The red lines are the sum of zero-point vibrational energy and kT (0.596 kcal/mol). (c) The distance between proton and O of GLU198 in the 40 to 60 ps QM/MM MD simulation. (d) Snapshots of tubulin-PAC complex along the dynamic simulation time. For clarity, the water molecules have been removed. The distances between protonated and the O atom/N atom are marked in the figure.

Figure 6
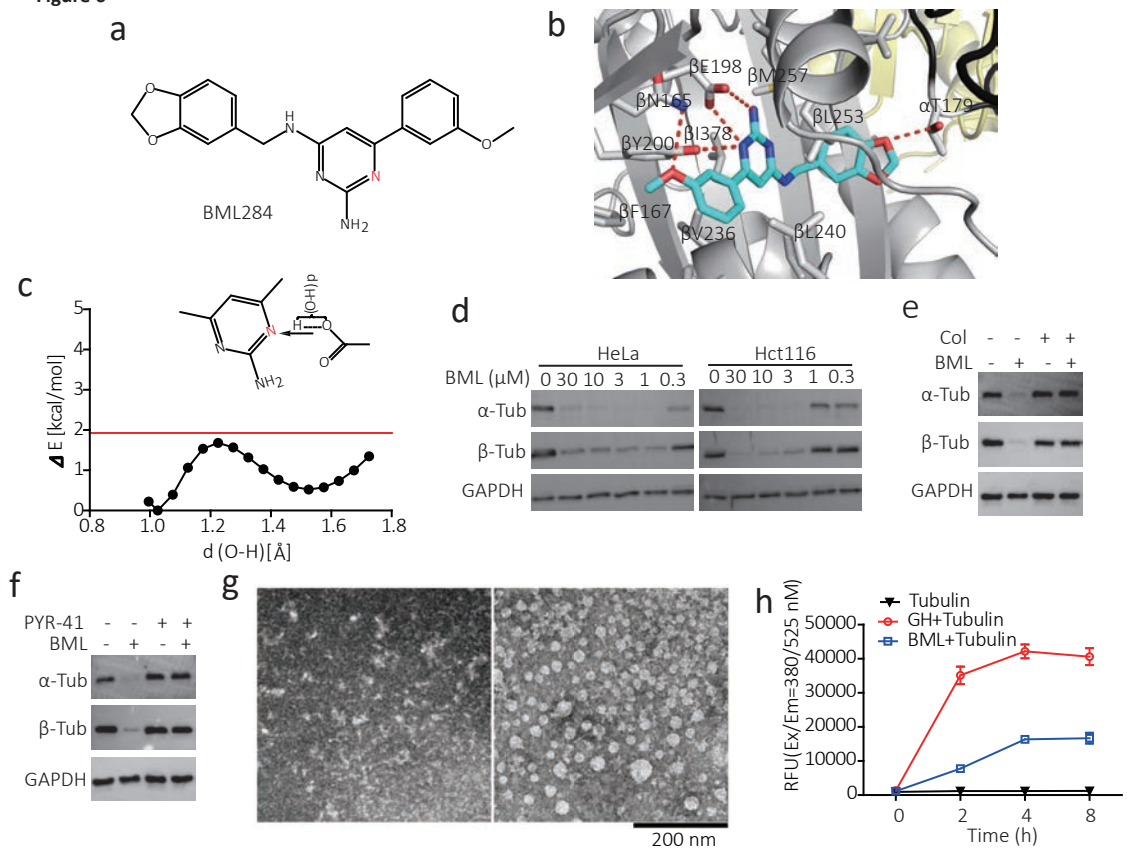
Figure 6: Identification of a new tubulin degrader with the LBHB mediated degradation mechanism. (**a**) Chemical structure of BML284. (**b**) Interactions between BML284 and tubulin. Residues that make interactions with BML284 are shown as sticks and are labeled. Hydrogen bonds are drawn with red dashed lines. (**c**) Energy profiles along the proton transfer coordinate for H-bond donor-acceptor pairs of the indicated hydrogen bond in tubulin-BML284 complexes. The red line is the sum of zero-point vibrational energy and kT (0.596 kcal/mol). (**d**) Immunoblot analysis of α- and β-tubulin protein levels in HeLa, Hct116 cells treated with the indicated concentrations of BML284 for 24 h. GAPDH was used as loading control. Results are representative of three independent experiments. (**e**) Colchicine blocks BML284-induced tubulin degradation. HeLa cells were pretreated with 3μM colchicine for one hour before treated with 3μM BML284 for 16 hours and then subjected to immunoblot analysis of α- and β-tubulin protein. Results are representative of three independent experiments. (**f**) Ubiquitin inhibitor PYR-41 rescue BML284-induced tubulin degradation. HeLa cells were pretreated 20 μM PYR-41 for one hour before treated with BML284 for 16 hours and then subjected to immunoblot analysis of α- and β-tubulin protein. Results are representative of three independent experiments. (**g**) Purified porcine tubulin (10 μM) was incubated with or without 20μM BML284 for 4 hours at room temperature, the images were taken by TEM. Results are representative of two independent experiments. (**h**) BML284 promotes purified tubulin denaturation. Tubulin (1μM) was incubated with guanidine hydrochloride（GH）or BML284 for 2, 4 or 8hours at room temperature. Then master reaction mix was added to the samples and incubated for another 30min. At last the fluorescent adduct were detected by a Biotech Gen5 spectrophotometer (λex = 380/λem = 525 nm). Data are shown as the mean ± SD (n = 3).
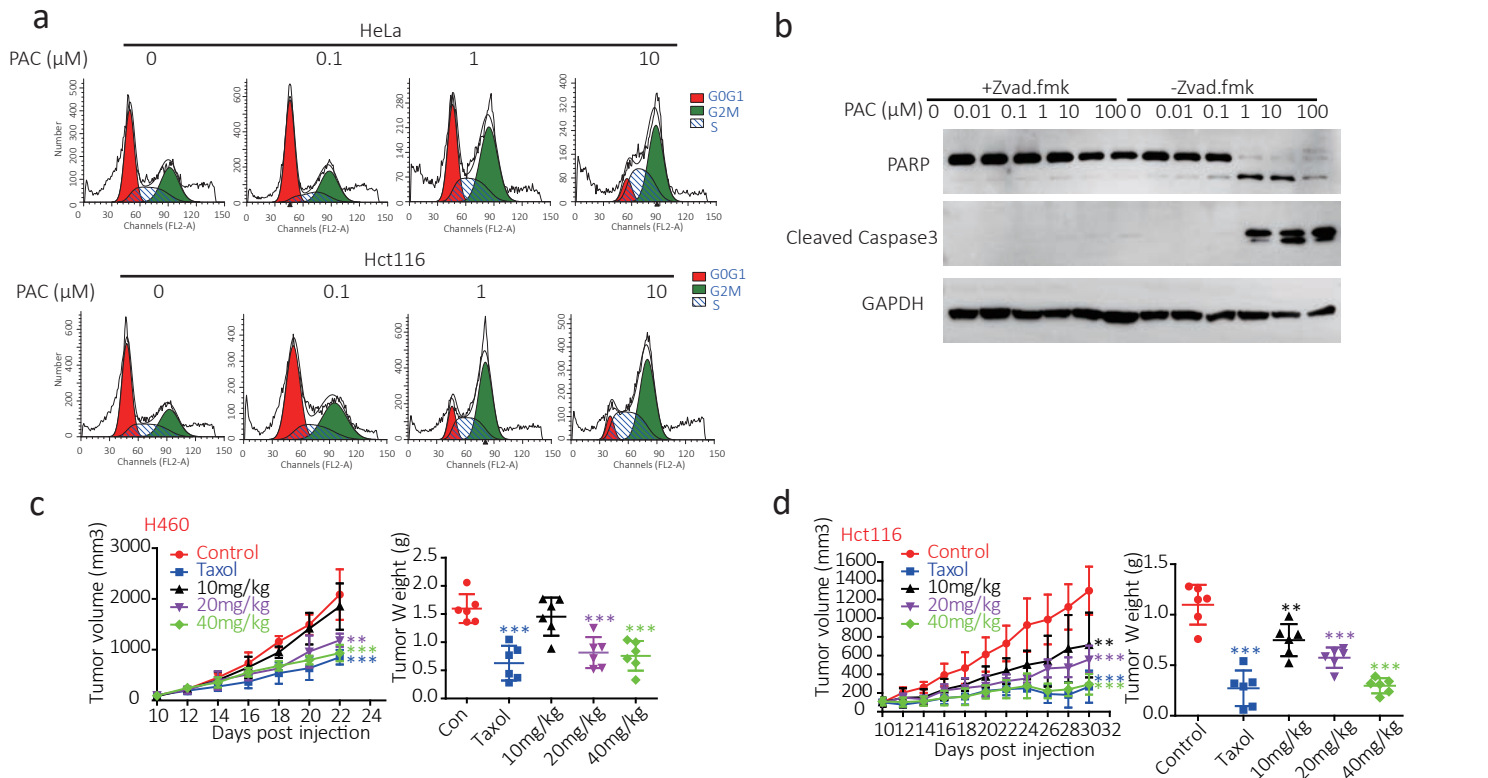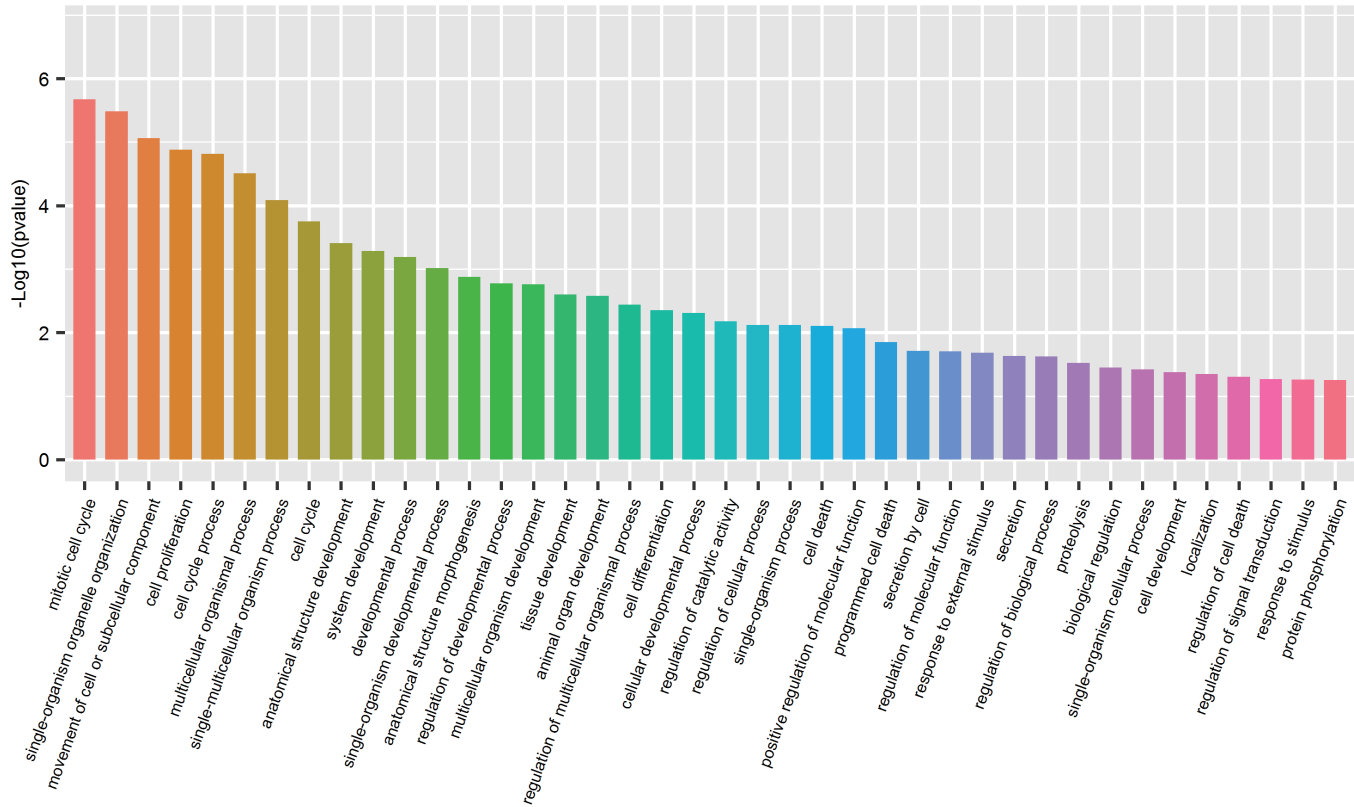
Figure S1

Figure S1: PAC induces G2/M phase cell cycle arrest and apoptosis and exhibits in vivo anticancer activity. (**a**) Flow cytometric histograms of various concentrations of PAC treated HeLa and Hct116 cells stained with propidium iodide. Results are representative of two independent experiments. (**b**) HeLa cells were treated with or without pan-caspase inhibitor Zvad.fmk for 1 hour before treated various concentrations of PAC for 48hous, then expression of poly ADP-ribose polymerase (PARP) and cleaved-caspase 3 were detected by immunoblot. GAPDH was loading control. Results are representative of two independent experiments. (**c**) In vivo antitumor activity of PAC (two days a time, tail vein injection) and taxol (30mg/kg, once a week，intraperitoneal injection) against H460 xenografts. Left: Time curve of tumor growth. Points showed as mean ± SD (n=6). Right: Bar chart of tumor weight. (**d**) In vivo antitumor activity of PAC (two days a time, tail vein injection) and taxol (30mg/kg, once a week，intraperitoneal injection) against Hct116 xenografts. Left: Time curve of tumor growth. Points showed as mean ± SD (n=6). Right: Bar chart of tumor weight.
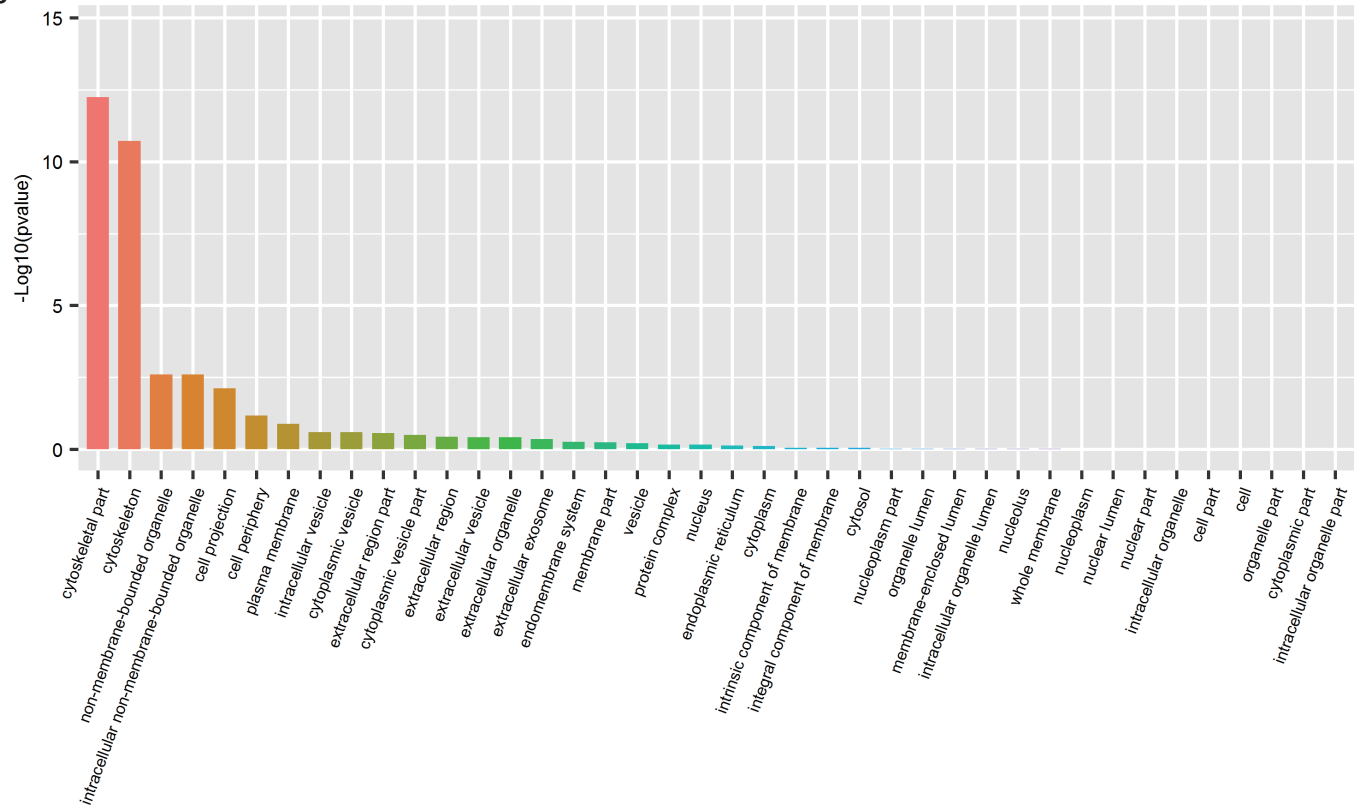
Figure S2: Biological processes and cellular components analysis of the quantitative proteomic data. (**a**) Rank order list of the most statistically enriched biological processes changes by PAC (Go Enrichment Analysis of biological processes) (**b**) Rank order list of the most statistically enriched cellular components changes by PAC (Go Enrichment Analysis of components changes).
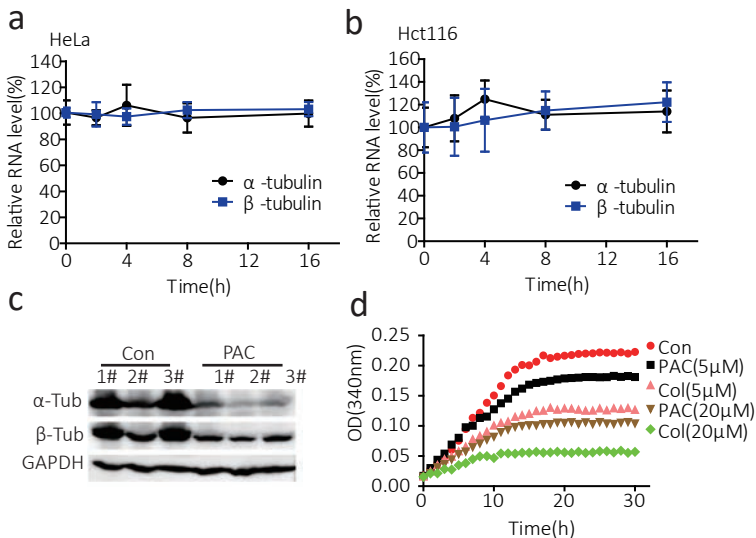
Figure S3

Figure S3: Supplementary figure for PAC induced tubulin degradation. (**a, b**) Time course of α- and β-tubulin mRNA levels in (**a**) HeLa and (**b**) Hct116 cells treated with 1 μM PAC or DMSO. Results are shown as the mean ± SD (n = 3). (**c**) Analysis of tubulin protein levels of Hct116 xenograft tissue. Tumor bearing mice were administrated with PAC at the dose of 80 mg/kg once through tail veil injection. Then mice were sacrificed after 24hours and xenograft tissues were collected for immunoblot to detect α- and β-tubulin protein. Results are representative of two independent experiments. (**d**) Indicated concentrations of compounds were co-incubated with tubulin（3mg/ml）at 37℃, absorbance at 340 nm were detected every one minutes for 30 minutes. Results are representative of two independent experiments.

Figure S4
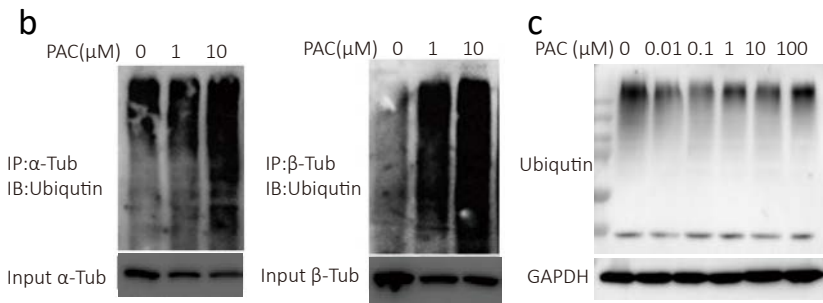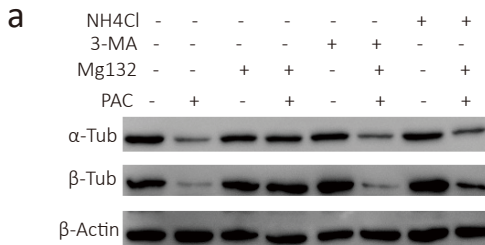
Figure S4: PAC promotes ubiquitin- and proteasome-dependent degradation of tubulins.
(**a**) Chemical rescue of PAC induced tubulin degradation. HeLa cells were pretreated with
Mg132, NH4Cl or 3-MA for 1hours before treated with PAC. Results are representative of
three independent experiments. (**b**) HeLa cells were treated with 0, 1or 10μM PAC for 6hours,
α- or β-tubulin were immunoprecipitated from the lysates, and ubiquitinylated α- or
β-tubulin were detected with anti-ubiquitin antibodies. Results are representative of three
independent experiments. (**c**) HeLa cells were treated with indicated concentrations of PAC for
16hours, then total protein was extracted and analyzed by immunoblot for ubiquitin.
Results are representative of two independent experiments.
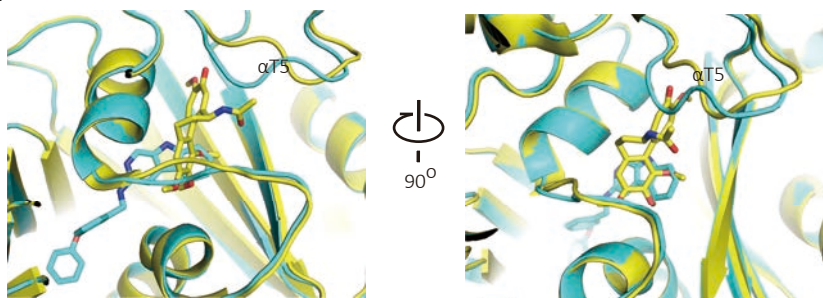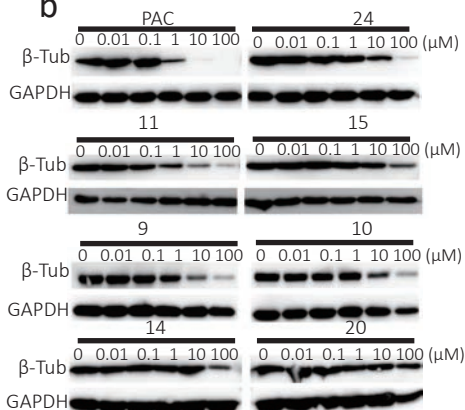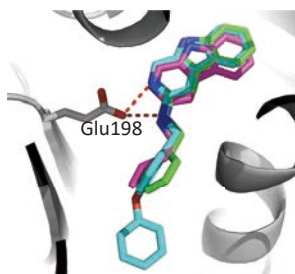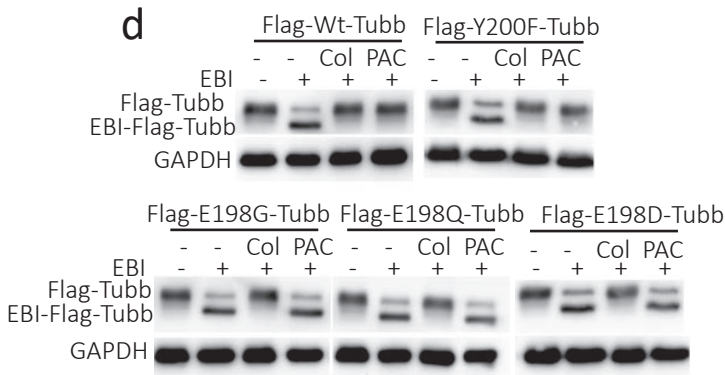
Figure S5: Supplementary figure to support an LBHB between PAC and βGlu198 mediates tubulin degradation. (**a**) Comparison of the tubulin binding modes between PAC and colchicine. The complex structures of tubulin–PAC (cyan) and Tubulin-colchicine (PDB ID: 4O2B, yellow) are superimposed. (**b**) Tubulin degradation activity of PAC derivatives. HeLa cells were treated with different concentrations of indicated compound for 16 hours, the β-tubulin protein levels were monitored by immunoblot. Results are representative of two independent experiments. (**c**) Comparison of the tubulin binding modes of PAC, compound 9 and 11. The structures of tubulin complexed with PAC (blue), compound 9 (green) and compound 11 (purple) are superimposed. (**d**) Identification the binding of PAC to wild type or mutant tubulins by EBI competition assay. MSCV-IRES-GFP vectors expressing both EGFP and wild type or mutant Flag-β-tubulin were transfected to HeLa cells for 24 hours. Then cells were treated with 10μM colchicine and 10μM PAC for 2hours before treated with 100μM EBI for another 2hours. Flag-β-tubulin level were detected by immunoblot. Results are representative of two independent experiments.
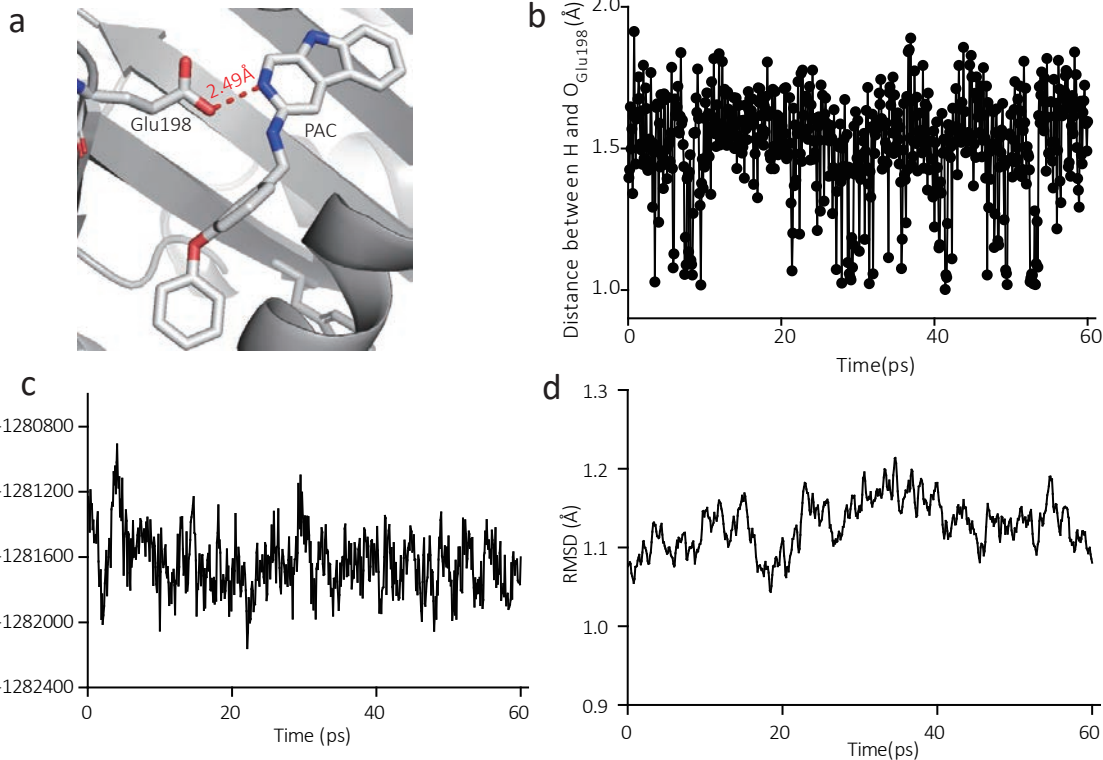
Figure S6

Figure S6: **QM/MM MD simulation results.** (**a**) Close-up view of the interaction between β Glu198 with PAC in QM/MM optimized structure showed the distance of the OGlu198-NPAC hydrogen bond. (**b**) The distance between proton and O of Glu198 in the 0 to 60 ps QM/MM MD simulation. (**c**) The total potential energy of the 0 to 60ps trajectory for PAC-tubulin complex. (**d**) Root mean square deviations (RMSDs) for 0 to 60 ps QM/MM MD simulation (QM: B3LYP/6-31G).
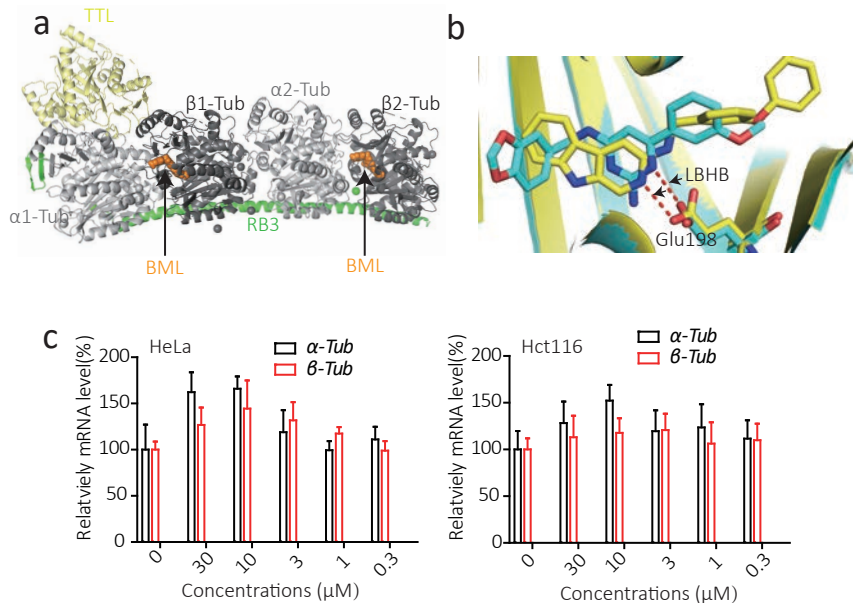
Figure S7: Supplementary figures to support BML284 induces tubulin degradation with the LBHB mediating degradation mechanism. (a) Overall structure of tubulin-BML284 crystal complex. The RB3-SLD is colored green, TTL is yellow, α-tubulin is grey, β-tubulin is black, BML284 is orange and shown as spheres. (b) Comparison of the tubulin binding modes of PAC and BML284. The structures of tubulin complexed with PAC (cyan) and BML284 (yellow) are superimposed. (c) The relative mRNA levels of α- and β-tubulin in HeLa and Hct116 cells treated with indicated concentrations of BML284 for 16hours were tested by Quantitative PCR, and the data are shown as the mean ± SD (n = 3).